High-pressure ethanol oxidation and its interaction with NO

Lorena Marrodán, Álvaro J. Arnal, Ángela Millera, Rafael Bilbao, María U. Alzueta*

Aragón Institute of Engineering Research (I3A). Department of Chemical and Environmental Engineering.

University of Zaragoza. C/ Mariano Esquillor, s/n. 50018 Zaragoza. Spain

*uxue@unizar.es

ABSTRACT

Ethanol has become a promising biofuel, widely used as a renewable fuel and gasoline additive. Describing the oxidation kinetics of ethanol with high accuracy is required for the development of future efficient combustion devices with lower pollutant emissions. The oxidation process of ethanol, from reducing to oxidizing conditions, and its pressure dependence (20, 40 and 60 bar) has been analyzed in the 500-1100 K temperature range, in a tubular flow reactor under well controlled conditions. The effect of the presence of NO has been also investigated. The experimental results have been interpreted in terms of a detailed chemical kinetic mechanism with the GADM mechanism (*Glarborg P, Alzueta MU, Dam-Johansen K and Miller JA, 1998*) as a base mechanism but updated, validated, extended by our research group with reactions added from the ethanol oxidation mechanism of Alzueta and Hernández (*Alzueta MU and Hernández JM, 2002*), and revised according to the present high-pressure conditions and the presence of NO. The final mechanism is able to reproduce the experimental trends observed on the reactants consumption and main products formation during the ethanol oxidation under the conditions studied in this work. The results show that the oxygen availability in the reactant mixture has an almost imperceptible effect on the temperature for the onset of ethanol consumption at a constant pressure, but this consumption is faster for the highest value of air excess ratio (λ) analyzed. Moreover, as the pressure becomes higher, the oxidation of ethanol starts at lower temperatures. The presence of NO promotes ethanol oxidation, due to the increased relevance of the interactions of CH_3 radicals and NO_2 (from the conversion of NO to NO_2 at high pressures and in presence of O_2) and the increased concentration of OH radicals from the interaction of NO_2 and water.

Keywords: ethanol; oxidation; high-pressure; nitrogen oxides; modeling.

1. Introduction

Minimizing particulate matter and nitrogen oxides (NO_x) emissions from combustion, especially from transport, is a pressing need to improve the air quality, preserve the environment and comply with the increasingly restrictive laws. A prospective solution is fuel reformulation since its effects on emissions are immediate and can be implemented, without significant changes, in the design of the equipment. This reformulation implies the total or partial replacement of the conventional fuel by alternative ones, that may have been obtained in a more environmentally friendly way, for example, alcohols such as ethanol or butanol from biomass or wastes by biorefinery processes [1].

Ethanol (C_2H_5OH) is one of the most studied alcohols and its use, directly or as a gasoline additive, is spread worldwide. However, the cetane number, flash point and calorific value of ethanol are lower than those corresponding to diesel fuel, so it cannot be used directly in diesel engines. Therefore, ethanol must be blended with diesel fuel or biodiesel [2] and, working under the appropriate conditions, the emissions of CO, particulate matter and NO_x could be reduced [3].

The ethanol oxidation has been investigated in several works using laminar flames, shock tubes, flow reactors and rapid compression machines, as it has been summarized in the study of Mittal et al. [4]. More recently, Barraza-Botet et al. [5] carried out ignition and speciation studies in ethanol combustion in a rapid compression facility. For modeling predictions, they [5] used the detailed mechanism of Burke et al. [6,7] developed for C_1-C_3 hydrocarbons and oxygenated species oxidation, obtaining a good agreement with the experimental results.

However, despite its relevance for its applicability to internal combustion engines, the ethanol oxidation in flow reactors under high-pressure conditions has not been previously studied. Therefore, reliable experimental data for validation of the kinetic models in this high-pressure regime become of high importance.

In this context, the aim of the present work is to extend the experimental database on ethanol oxidation with the study of its conversion under high-pressure conditions, in a flow reactor, for different air excess ratios, both in the absence and presence of nitric oxide (NO). NO may be formed in the combustion chamber of a diesel engine, mainly through the thermal NO mechanism and, once it has been formed, NO may

interact with ethanol or its derivatives. The experimental results are analyzed in terms of a detailed chemical kinetic mechanism to identify the main reaction routes occurring and to better understand the possible ethanol-NO interactions.

2. Experimental methodology

The ethanol oxidation experiments, both in the absence and presence of NO, have been carried out in a high-pressure flow reactor designed to approximate gas plug flow. The experimental set up is described in detail in Marrodán et al. [8] and only a brief description is provided here. A controlled evaporator mixer (CEM) has been used to feed an aqueous solution of ethanol (10% by weight) into the reaction system. The oxygen required to carry out each oxidation experiment depends on the air excess ratio analyzed (λ, defined as the inlet oxygen concentration divided by stoichiometric oxygen), and it has been supplied from gas cylinder through a Bronkhorst Hi-Tech mass flow controller. In the case of the experiments in the presence of NO, 500 ppm of NO have been added to the feed gas flow. Table 1 lists the conditions of the different experiments.

The gas reactants are premixed before entering the reaction system, which consists of a tubular quartz reactor (inner diameter of 6 mm and 1500 mm in length) enclosed in a stainless-steel tube that acts as a pressure shell. The longitudinal temperature profile in the reactor was experimentally determined. An isothermal zone (±10 K) of 56 cm was obtained in the reactor, which was considered as reaction zone. Nitrogen to balance up to obtain a total flow rate of 1 L (STP)/min has been used, resulting in a gas residence time dependent of the pressure and the temperature according to: t_r (s)=261 P(bar)/T(K).

The products were analyzed using an on-line 3000A Agilent micro-chromatograph equipped with TCD detectors and an URAS26 ABB continuous IR NO analyzer. The uncertainty of the measurements is estimated as ±5%, but not less than 10 ppm.

3. Modeling

Simulations of the experimental results obtained in the ethanol high-pressure oxidation, in the absence and presence of NO, have been made using a gas-phase chemical kinetic model and the software Chemkin-Pro

[9]. The detailed mechanism used in this work has been built up by our research group from the GADM mechanism [10], progressively updated (e.g. [11,12]) and modified to consider the different experimental conditions, such as the high-pressure and/or the different compounds involved [13-17]. In the case of ethanol, the reaction subset proposed by Alzueta and Hernández [18] in an atmospheric ethanol oxidation study has been included in the mechanism compiled in this work. Formic acid (HCOOH) has been identified as an intermediate in oxidation of dimethyl ether [19], which is an isomer of ethanol, so the reaction subset for formic acid oxidation proposed by Marshall and Glarborg [20] has also been included in the mechanism. The thermodynamic data for the species involved are taken from the same sources as the original mechanisms. The complete mechanism (137 species and 798 reactions) is provided as Supplementary Material in CHEMKIN format.

4. Results and discussion

A study of ethanol oxidation at high pressure (20, 40 and 60 bar), in the 500-1100 K temperature range, has been carried out, for different air excess ratios (λ=0.7, 1 and 4), both in the absence and in the presence of NO.

4.1. Oxidation of ethanol in the absence of NO

Figure 1 shows an example of the results for ethanol consumption and CO and CO_2 formation as a function of temperature for the conditions of set 4 in Table 1, i.e., 20 bar, stoichiometric conditions (λ=1) and in the absence of NO. From now on, experimental results are denoted by symbols, and modeling calculations by lines. In general, there is a good agreement between the experimental results and model predictions. Under these conditions, the ethanol conversion starts at approximately 725 K, the same temperature as for the onset of CO formation whose concentration peaks at 775 K. At the highest temperatures, ethanol and CO are completely oxidized to CO_2.

Figure 2 shows the concentration of ethanol and of the main products quantified (CO, CO_2, CH_3CHO, C_2H_4, CH_4, CH_3OH, H_2), for different air excess ratios (from λ=0.7 to λ=4), at a constant pressure of 20 bar, and in the absence of NO. The oxygen availability in the reactant mixture does not modify significantly the

109 temperature for the onset of ethanol conversion at a given pressure. In an ethanol oxidation study at
110 atmospheric pressure, Alzueta and Hernández [18] observed that the ethanol oxidation occurs at lower
111 temperatures for very oxidizing conditions (λ=35), and small differences between λ=0.7 and λ=1 were found.
112 The biggest discrepancies can be found in the experimental and modeling results for CH_4, for reducing and
113 stoichiometric conditions, and CH_3OH, minor products compared to CO and CO_2. The same tendencies can
114 be observed for the other pressures studied in this work, although these results are not shown.
115 In order to further evaluate the influence of air excess ratio on ethanol oxidation, given the little influence
116 found for λ=1 and λ=4, model calculations for λ=35, very fuel-lean conditions, have been carried out. The
117 theoretical results obtained for λ=35 (Figure 2) are almost the same than those for λ=4, for ethanol,
118 acetaldehyde (CH_3CHO) and CO and CO_2 concentrations, but lower amounts of CH_4, C_2H_4 and CH_3OH are
119 predicted. So, it can also be deduced that for the high-pressure conditions studied in this work, there is
120 almost no influence of the oxygen availability on the temperature for the onset of ethanol oxidation.
121 Figure 3 shows the influence of the pressure change (20, 40 and 60 bar) on the ethanol consumption and CO
122 formation, which has been selected as one of the main products of ethanol oxidation. Independently of the
123 stoichiometry analyzed, the consumption of ethanol starts at lower temperatures as the pressure is
124 increased, approximately 100 K when moving from 20 to 60 bar. This behavior is also observed in the
125 formation of CO, which peaks at lower temperatures for the highest pressure analyzed. The oxidation of CO
126 to CO_2 is favored by an increase in pressure, as well as by an increase in the lambda value.
127 Considering the experimental procedure utilized in this work, a change in the pressure maintaining the total
128 gas flow rate, also implies a change in the gas residence time (t_r (s)=261 P(bar)/T(K)). Therefore, with the
129 present mechanism, that describes well the experimental results, we have made different simulations to try
130 to distinguish between the effect of gas residence time or pressure. This evaluation can be found as
131 Supplementary Material, Figure S.1. The results indicate that both the pressure and the residence time have
132 an appreciable effect on the ethanol conversion, which is shifted to lower temperatures when any of the
133 above variables is increased. Accordingly, the results presented in Figure 3 correspond to the joint effect of
134 pressure and residence time.

In general, modeling predictions are in good agreement with the experimental observations. Consequently, in this work, reaction rate analysis has been performed to identify the main ethanol consumption routes and products formation and the obtained results have been represented in a reaction pathway diagram in Figure 4 (left).

The ethanol consumption is initiated by its thermal dehydration to ethylene (reaction R.1), as this latter has been detected by gas chromatography, and also by its thermal decomposition through bond cleavage to CH_2OH and CH_3 radicals (reaction R.2). For example, for 20 bar and λ=0.7, at 725 K, 86% of the ethanol is being consumed through reaction R.2, and for λ=4, 95% of the ethanol consumption is produced through reaction R.1. This fact could explain the almost negligible effect of the oxygen availability on the temperature for the onset of ethanol consumption.

$$C_2H_5OH(+M) \rightleftharpoons C_2H_4 + H_2O(+M) \qquad \text{(R.1)}$$

$$C_2H_5OH(+M) \rightleftharpoons CH_2OH + CH_3(+M) \qquad \text{(R.2)}$$

In earlier studies involving ethanol oxidation in flow reactors [18,21], and in flames and jet stirred reactors [22], the main reaction pathways for ethanol consumption were identified. The proposed reaction routes are based on a hydrogen abstraction that may occur on three different sites, leading to the formation of three different C_2H_5O radical isomers (reaction R.3, where R can be O, H, OH, CH_3 or HO_2 radicals).

$$C_2H_5OH + R \rightleftharpoons CH_3CHOH/CH_2CH_2OH/CH_3CH_2O + RH \qquad \text{(R.3)}$$

Under the conditions of the present work, these reactions also take place, especially that one involving HO_2 radicals, as it was previously observed in the oxidation of other oxygenated compounds, such as dimethoxymethane [23], under high-pressure conditions. The hydroxymethyl radical (CH_2OH), formed in reaction R.2 from ethanol, reacts with molecular oxygen to produce formaldehyde and more HO_2 radicals (reaction R.4), which interact with ethanol (reaction R.3) producing the CH_3CHOH radical, the dominant radical under the present conditions.

$$CH_2OH + O_2 \rightleftharpoons CH_2O + HO_2 \qquad \text{(R.4)}$$

An example of the evolution along the reactor of the main consumption reactions for ethanol can be observed in Figure 4 (right), for 20 bar, λ=1 and 725 K. At the beginning of the reactor, the ethanol

consumption is mainly through its thermal dehydration (reaction R.1), but hydrogen abstraction reaction by HO_2 (reaction R.3) becomes more relevant with the distance.

The CH_3CHOH radical reacts with molecular oxygen (reaction R.5) producing acetaldehyde, which has been quantified by gas chromatography. Acetaldehyde interacts with the radical pool producing the acetyl radical (CH_3CO), which thermally decomposes to CO and CH_3 radicals.

$$CH_3CHOH + O_2 \rightleftharpoons CH_3CHO + HO_2 \qquad \text{(R.5)}$$

The reaction pathways involving the other two C_2H_5O radicals are of minor relevance compared to those already described, and very similar to those described in previous ethanol oxidation works (e.g. [22]).

As it has been mentioned in the introduction, the mechanism of Burke et al. [6,7] has been used in previous ethanol studies, e.g. [5]. Therefore, it has been considered interesting to compare the experimental results obtained in this work with those predicted with the present model and the Burke et al. model. This comparison can be found as Supplementary Material, Figures S2-S10.

It can be observed that, in general, the model proposed in this work fits better the experimental results corresponding to the ethanol conversion onset temperature and the concentrations of ethanol, CO, CO_2, H_2 and C_2H_4, while the Burke et al. model fits better the concentrations corresponding to CH_4 and CH_3OH.

4.2. Oxidation of ethanol in the presence of NO

In the present work, the influence of the presence of NO in the reactant mixture on ethanol oxidation has also been analyzed. When burning any fuel in an air atmosphere at high temperatures, NO may be formed through the thermal NO formation mechanism by nitrogen fixation from the combustion air [24]. NO may be reduced by its interaction with ethanol and/or its derivatives, or may promote the ethanol oxidation in a mutually sensitized oxidation [25]. Therefore, the interaction between ethanol and NO has been considered in the present work from both experimental and modeling points of view.

As it can be drawn from the discussion of the main reaction pathways for ethanol conversion in the absence of NO, a high concentration of CH_3 radicals is also expected in the presence of NO. Furthermore, under the present experimental conditions, it has been observed that, due to the high-pressure conditions and the presence of O_2, NO added to the reactant mixture is converted to NO_2 before entering the reactor. From the

188 interaction between CH_3 radicals and NO_2 (reaction -R.6), the mechanism initially compiled in this work
189 predicted an accumulation of nitromethane (CH_3NO_2), whose formation was not detected experimentally.
190 Another possible interaction between CH_3 radicals and NO_2 leading to CH_3ONO may occur (reaction -R.7).

191 $$CH_3 + NO_2(+M) \rightleftharpoons CH_3NO_2(+M) \qquad (-R.6)$$

192 $$CH_3 + NO_2 \rightleftharpoons CH_3ONO \qquad (-R.7)$$

193 In a high-pressure flow reactor study, Rasmussen and Glarborg [16] analyzed the effects of NO_x on CH_4
194 oxidation, through ab initio calculations. Their calculations indicated that the formation of CH_3ONO is
195 energetically unfavorable, but, if formed, it would dissociate to NO and methoxy radical (CH_3O).
196 Therefore, because of the high CH_3 and NO_2 concentrations expected and no CH_3NO_2 detection, the CH_3ONO
197 reaction to CH_3 and NO_2 (reaction R.7) has been included in our mechanism. There is not much information
198 in bibliography regarding this reaction and its kinetic parameters. So, the value of 7.00×10^{10} cm^3 mol^{-1} s^{-1}
199 proposed by Canosa et al. [26] has been adopted for reaction R.7. As it can be seen in Figure 5, in the
200 concentration profiles of ethanol and CO, the predictions of the model improved considerably after including
201 reaction R.7 in the mechanism.
202 Figure 6 (top) shows a comparison between the experimental results (symbols) and model predictions (lines)
203 obtained during ethanol oxidation, in the presence of NO, for different air excess ratios and different
204 pressures. Compared to Figure 3, the presence of NO promotes ethanol oxidation shifting the onset of
205 ethanol oxidation to lower temperatures, a difference of 100-125 K approximately. As also occurred in the
206 absence of NO, the available oxygen in the reactant mixture does not modify the temperature for the onset
207 of ethanol conversion at a constant pressure of 20 bar. The same tendency was observed for the other
208 pressures analyzed (results not shown), but the higher the pressure the lower the ethanol conversion onset
209 temperature. Figure 6 (bottom) shows the experimental and theoretical NO concentration results for
210 different air excess ratios and 20 bar, and also other pressures for λ=4. Modeling predictions are shifted to
211 higher temperatures, approximately 50 K, compared to experimental results. At low temperatures, as
212 previously mentioned, the NO fed to the system is converted to NO_2 through reaction R.8, and it is not thus
213 experimentally detected until approximately 750 K. Unlike what was observed for ethanol, both λ and

pressure values influence the NO concentration, in the way that increasing the amount of oxygen in the reactant mixture or increasing the pressure, results in a lower amount of NO experimental or predicted.

$$2NO + O_2 \rightleftharpoons 2NO_2 \quad \text{(R.8)}$$

Once formed, NO_2 reacts with CH_3 radicals originated from ethanol to produce CH_3ONO (reaction -R7), which decomposes rapidly into CH_3O+NO. As a consequence, NO is detected again, especially for 20 bar and λ=0.7, because an increase in the value of pressure or lambda favors reaction R.8.

NO_2 can also react with H_2O to produce HONO and OH radicals (reaction R.9), which promote ethanol conversion. The HONO formed decomposes to produce NO (reaction R.10).

$$NO_2 + H_2O \rightleftharpoons HONO + OH \quad \text{(R.9)}$$

$$HONO(+M) \rightleftharpoons NO + OH(+M) \quad \text{(R.10)}$$

The same reactions (R.9 and R.10), but in the reverse sense, were the cause of a slightly inhibiting effect of ethanol conversion by NO observed in the ethanol oxidation at atmospheric pressure [18], under certain conditions.

In the presence of NO, the ethanol consumption routes are the same as those already described in the absence of NO. However, in the presence of NO, the reaction pathways involving the CH_3CH_2O radical (formed through R.3) acquire more relevance, becoming the predominating reaction pathways. This radical decomposes through reactions R.11 and R.12 to produce acetaldehyde or CH_3 radicals and formaldehyde, respectively.

$$CH_3CH_2O + M \rightleftharpoons CH_3CHO + H + M \quad \text{(R.11)}$$

$$CH_3CH_2O + M \rightleftharpoons CH_3 + CH_2O + M \quad \text{(R.12)}$$

First-order sensitivity analyses for ethanol and CO have been performed for different air excess ratios and 20 bar, in the absence of NO and in the presence of NO.

The obtained ethanol results are in agreement with the ethanol consumption pathways previously described and can be found as Supplementary Material, Figure S11. In the absence of NO, the most sensitive reaction is the hydrogen abstraction reaction by HO_2 (reaction R.3), which is the main reaction pathway for ethanol consumption. The reaction H_2O_2(+M)=OH+OH(+M) is also very sensitive due to the generation of OH radicals

240 which can promote the consumption of ethanol by H abstraction reactions. In the presence of NO, the
241 formation of CH_3CH_2O radical from ethanol (reaction R.3, $C_2H_5OH+OH=CH_3CH_2O+H_2O$) and its thermal
242 decomposition (reactions R.11 and R.12) present a high sensitivity coefficient, becoming the dominant
243 ethanol consumption under these conditions. The CH_3 radicals generated in reaction R.12 may interact with
244 ethanol promoting its consumption. The formation of HONO from the interaction of CH_2O+NO_2
245 ($CH_2O+NO_2=HCO+HONO$) and its subsequent decomposition (reaction R.10, $HONO(+M)=NO+OH(+M)$)
246 producing OH radicals are sensitive in the presence of NO, because of the OH radicals generated that
247 promote ethanol conversion.
248 Moreover, the first-order sensitivity analysis for CO (Figure 7) indicates that, in the absence of NO, the most
249 sensitive reaction is the thermal dehydration of ethanol to ethylene (reaction R.1). The subsequent reaction
250 of ethylene with O_2 presents a high sensitivity for all the values of lambda analyzed. Hydrogen abstraction
251 reactions from ethanol with different radicals are also sensitive. In the presence of NO, as in the case of the
252 sensitivity results for ethanol, hydrogen abstraction reactions by OH radicals to produce CH_3CH_2O radical and
253 its subsequent decomposition are highly sensitive. The interaction of NO_2 with CH_2O to produce HONO and
254 HCO presents the highest sensitivity coefficient for all the lambdas analyzed.
255

256 **5. Conclusions**

257 The oxidation of ethanol has been analyzed from both experimental and modeling points of view. The
258 influence on the process of the available oxygen in the reactant mixture (different air excess ratios: λ=0.7, 1
259 and 4), the change of pressure (20, 40 and 60 bar) and the presence or absence of NO has been analyzed in a
260 tubular flow reactor, in the 500-1100 K temperature range.
261 In general, there is a good agreement between experimental and modeling predictions. The results show
262 that, for the conditions studied in this work, at a constant pressure, the temperature for the onset of ethanol
263 oxidation is roughly independent of the amount of oxygen available in the reactant mixture, but the ethanol
264 conversion starts at lower temperatures as the pressure is increased. A reaction rate analysis indicates that
265 the ethanol consumption is mainly initiated by thermal dehydration or decomposition.

When NO is fed to the high-pressure system, it converts to NO_2 before entering in the reactor. In view of the high expected concentration of NO_2 and CH_3 radicals (from the ethanol conversion), the reaction $CH_3ONO \rightleftharpoons CH_3 + NO_2$ has been included in our mechanism, with clear improvements of the model predictions. In the presence of NO, the ethanol conversion is promoted due to the increased concentration of OH in the radical pool from the interaction of NO_2 and water. As observed in the absence of NO, the stoichiometry does not have a clear influence on the ethanol oxidation regime, whereas an increase in the pressure shifts the temperature for the onset of ethanol consumption to lower temperatures.

Acknowledgements

The authors express their gratitude to Aragón Government and European Social Fund (GPT group), and to MINECO and FEDER (Project CTQ2015-65226) for financial support. Ms. Marrodán acknowledges Aragón Government for the predoctoral grant awarded.

References

[1] Sarathy SM, Oßwald P, Hansen N, Kohse-Höinghaus K. Alcohol combustion chemistry. *Prog. Energy Combust. Sci.* 2014;44:40-102.

[2] Alviso D, Krauch F, Román R, Maldonado H, dos Santos RG, Rolón JC, Darabiha N. Development of a diesel-biodiesel-ethanol combined chemical scheme and analysis of reactions pathways. *Fuel* 2017; 191:411-426.

[3] An H, Yang WM, Li J. Effects of ethanol addition on biodiesel combustion: a modeling study. *Appl. Energy* 2015;143:176-188.

[4] Mittal G, Burke SM, Davies VA, Parajuli B, Metcalfe WK, Curran HJ. Autoignition of ethanol in a rapid compression machine. *Combust. Flame* 2014;161:1164-1171.

[5] Barraza-Botet CL, Wagnon SW, Wooldridge MS. Combustion chemistry of ethanol: ignition and speciation studies in a rapid compression facility. *J. Phys. Chem. A* 2016;120:7408-7418.

[6] Burke SM, Metcalfe W, Herbinet O, Batton-Leclerc F, Haas FM, Santner J, Dryer FL, Curran HJ. An experimental and modeling study of propene oxidation. Part 1: speciation measurements in jet-stirred and flow reactors. *Combust. Flame* 2014;161:2765-2784.

[7] Burke SM, Burke U, Mc Donagh R, Mathieu O, Osorio I, Keesee C, Morones A, Petersen EL, Wang W, DeVerter TA, et al. An experimental and modeling study of propene oxidation. Part 2: ignition delay time and flame speed measurements. *Combust. Flame* 2015;162:296-314.

[8] Marrodán L, Millera Á, Bilbao R, Alzueta MU. High-pressure study of methyl formate oxidation and its interaction with NO. *Energy Fuels* 2014;28:6107-6115.

[9] ANSYS Chemkin-Pro 17.2, Release 15151; Reaction Design: San Diego, 2016.

[10] Glarborg P, Alzueta MU, Dam-Johansen K, Miller JA. Kinetic modeling of hydrocarbon/nitric oxide interactions in a flow reactor. *Combust. Flame* 1998;115:1-27.

[11] Glarborg P, Alzueta MU, Kærgaard K, Dam-Johansen K. Oxidation of formaldehyde and its interaction with nitric oxide in a flow reactor. *Combust. Flame* 2003;132:629-638.

[12] Glarborg P, Østberg M, Alzueta MU, Dam-Johansen K, Miller JA. The recombination of hydrogen atoms with nitric oxide at high temperatures. *Proc. Combust. Inst.* 1999;27:219-227.

[13] Rasmussen CL, Hansen J, Marshall P, Glarborg P. Experimental measurements and kinetic modeling of $CO/H_2/O_2/NO_x$ conversion at high-pressure. *Int. J. Chem. Kin.* 2008;40:454-480.

[14] Rasmussen CL, Glarborg P. Measurements and kinetic modeling of CH_4/O_2 and $CH_4/C_2H_6/O_2$ conversion at high pressure. *Int. J. Chem. Kin.* 2008;40:778-807.

[15] Rasmussen CL, Andersen KH, Dam-Johansen K, Glarborg P. Methanol oxidation in a flow reactor: implications for the branching ratio of CH_3OH+OH reaction. *Int. J. Chem. Kin.* 2008;40:423-441.

[16] Rasmussen CL, Glarborg P. Sensitizing effects of NO_x on CH_4 oxidation at high pressure. *Combust. Flame* 2008;154:529-545.

[17] Giménez-López J, Rasmussen CT, Hashemi H, Alzueta MU, Gao Y, Marshall P, Goldsmith CF, Glarborg P. Experimental and kinetic modeling study of C_2H_2 oxidation at high pressure. *Int. J. Chem. Kin.* 2016;48:724-738.

[18] Alzueta MU, Hernández JM. Ethanol oxidation and its interaction with nitric oxide. *Energy Fuels* 2002;16:166-171.

[19] Fischer SL, Dryer FL, Curran HJ. The reaction kinetics of dimethyl ether. I: High-temperature pyrolysis and oxidation in flow reactors. *Int. J. Chem. Kinet.* 2000;32:713-740.

[20] Marshall P, Glarborg P. Ab initio and kinetic modeling studies of formic acid oxidation. *Proc. Combust. Inst.* 2015;35:153-160.

[21] Abián M, Esarte C, Millera Á, Bilbao R, Alzueta MU. Oxidation of acetylene-ethanol mixtures and their interaction with NO. *Energy Fuels* 2008;22:3814-3823.

[22] Leplat N, Dagaut P, Togbé C, Vandooren J. Numerical and experimental study of ethanol combustion and oxidation in laminar premixed flames and jet-stirred reactor. *Combust. Flame* 2011;158:705-725.

[23] Marrodán L, Royo E, Millera Á, Bilbao R, Alzueta MU. High-pressure oxidation of dimethoxymethane. *Energy Fuels* 2015;29:3507-3517.

[24] Abián M, Alzueta MU, Glarborg P. Formation of NO from N_2/O_2 mixtures in a flow reactor: toward and accurate prediction of thermal NO. *Int. J. Chem. Kinet.* 2015;47:518-532.

[25] Taylor PH, Cheng L, Dellinger B. The influence of nitric oxide on the oxidation of methanol and ethanol. *Combust. Flame* 1998;115:561-567.

[26] Canosa C, Penzhorn RD, Sonntag C. Product quantum yields from the photolysis of NO_2 at 366 nm in presence of ethylene. The role of NO^*_3. *Ber. Bunsenges Phys. Chem.* 1979;83:217-225.

Table captions

Table 1. Matrix of experimental conditions.

338 **Table 1.** Matrix of experimental conditions.

Set	Ethanol (ppm)	O_2 (ppm)	NO (ppm)	λ	P (bar)
1	5000	10500	0	0.7	20
2	5000	10500	0	0.7	40
3	5000	10500	0	0.7	60
4	5000	15000	0	1	20
5	5000	15000	0	1	40
6	5000	15000	0	1	60
7	5000	60000	0	4	20
8	5000	60000	0	4	40
9	5000	60000	0	4	60
10	5000	10500	500	0.7	20
11	5000	10500	500	0.7	40
12	5000	10500	500	0.7	60
13	5000	15000	500	1	20
14	5000	15000	500	1	40
15	5000	15000	500	1	60
16	5000	60000	500	4	20
17	5000	60000	500	4	40
18	5000	60000	500	4	60

339

340 **Figure captions**

341 **Figure 1.** Concentration of ethanol, CO and CO_2 as a function of temperature, for the conditions named as
342 set 4 in Table 1 (λ=1, 20 bar).

343

344 **Figure. 2.** Influence of the air excess ratio on the concentration profiles of ethanol and main products (CO,
345 CO_2, CH_3CHO, C_2H_4, CH_4, CH_3OH, H_2) during ethanol oxidation, as a function of temperature, for the
346 conditions named as sets 1, 4 and 7 in Table 1 (20 bar).

347

348 **Figure. 3.** Influence of the pressure change on the concentration profiles of ethanol and CO, as a function of
349 temperature, for the conditions named as sets 1-9 in Table 1.

350

351 **Figure 4.** Left: reaction path diagram for ethanol consumption and product formation. Right: normalized
352 rate-of-consumption coefficients for ethanol along the reactor (for the conditions of set 4 in Table 1: 20 bar,
353 λ=1 and 725 K).

354

355 **Figure 5.** Improvement in modeling predictions for ethanol and CO concentration, with and without reaction
356 R.7 in our mechanism, for the conditions named as set 16 in Table 1.

357

358 **Figure 6.** Influence of the air excess ratio and pressure on the concentration profiles of ethanol (top) and NO
359 (bottom) for the conditions named as sets 10, 13 and 16-18 in Table 1.

360

361 **Figure 7.** Sensitivity analysis for CO for different air excess ratios and 20 bar. Top: in the absence of NO (at
362 698 K). Bottom: in the presence of NO (at 648 K). (*) The sensitivity coefficients have been divided by two.

363

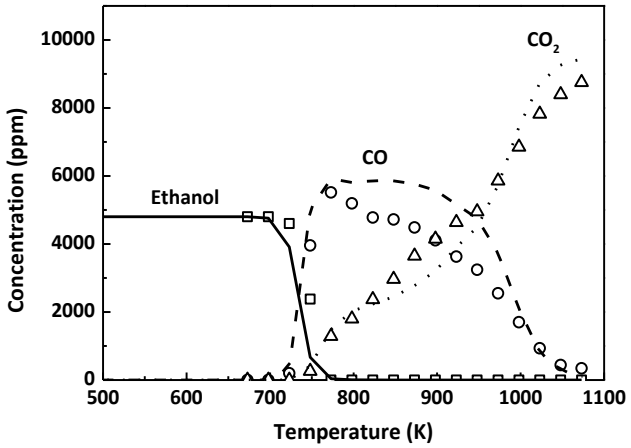

364

365 **Figure 1.** Concentration of ethanol, CO and CO_2 as a function of temperature, for the conditions named as

366 set 4 in Table 1 (λ=1, 20 bar).

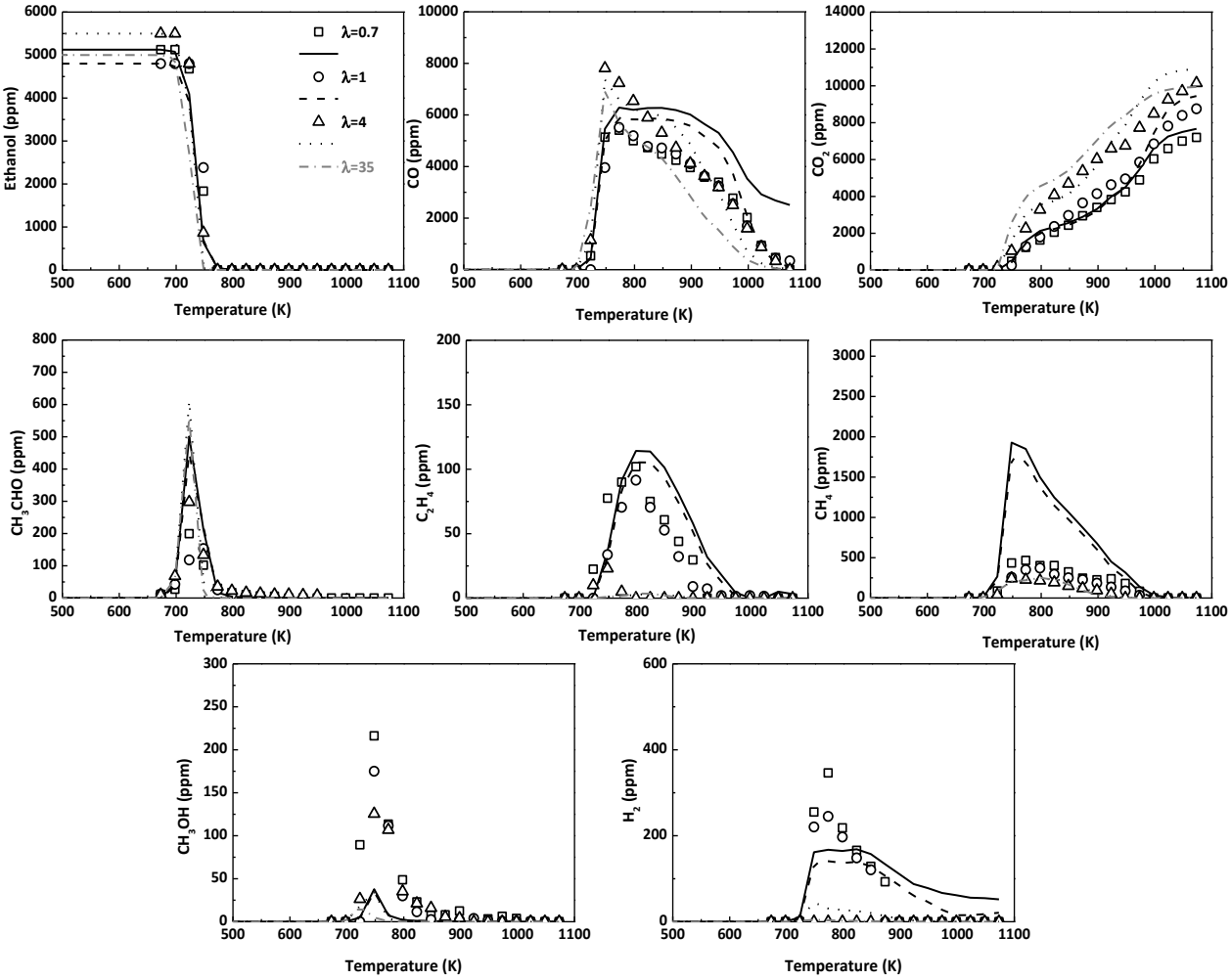

Figure. 2. Influence of the air excess ratio on the concentration profiles of ethanol and main products (CO, CO_2, CH_3CHO, C_2H_4, CH_4, CH_3OH, H_2) during ethanol oxidation, as a function of temperature, for the conditions named as sets 1, 4 and 7 in Table 1 (20 bar).

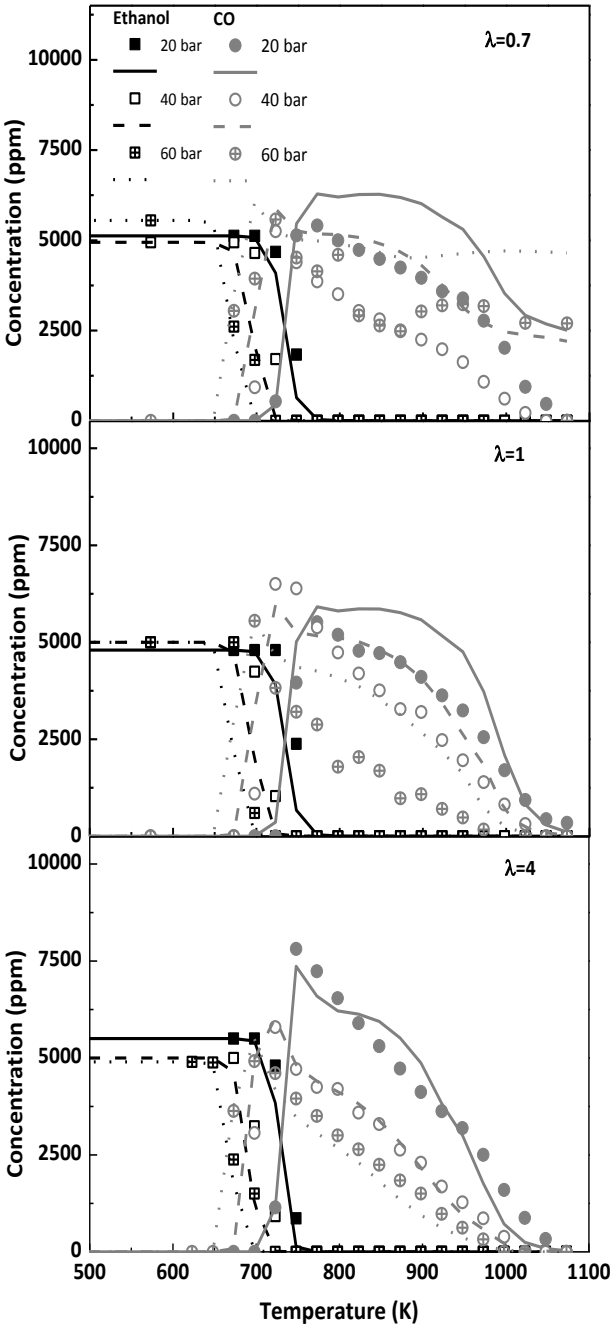

372 **Figure. 3.** Influence of the pressure change on the concentration profiles of ethanol and CO, as a function of

373 temperature, for the conditions named as sets 1-9 in Table 1.

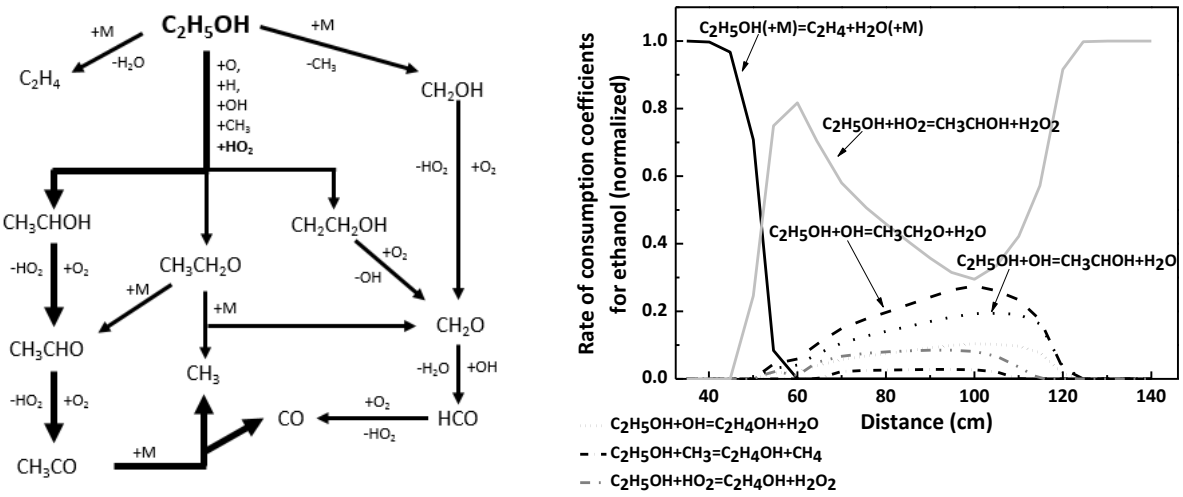

Figure 4. Left: reaction path diagram for ethanol consumption and product formation. Right: normalized rate-of-consumption coefficients for ethanol along the reactor (for the conditions of set 4 in Table 1: 20 bar, λ=1 and 725 K).

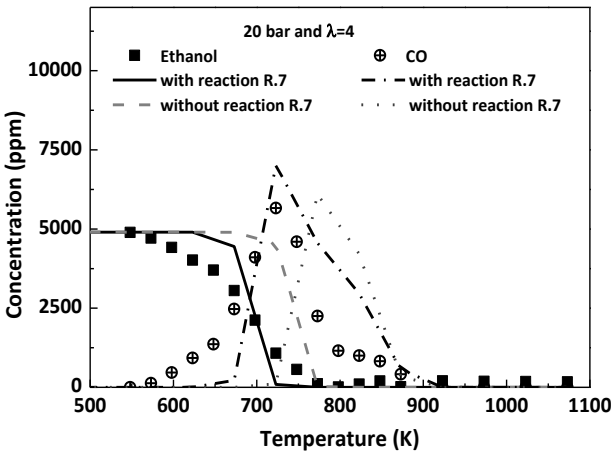

381 **Figure 5.** Improvement in modeling predictions for ethanol and CO concentration, with and without reaction

382 R.7 in our mechanism, for the conditions named as set 16 in Table 1.

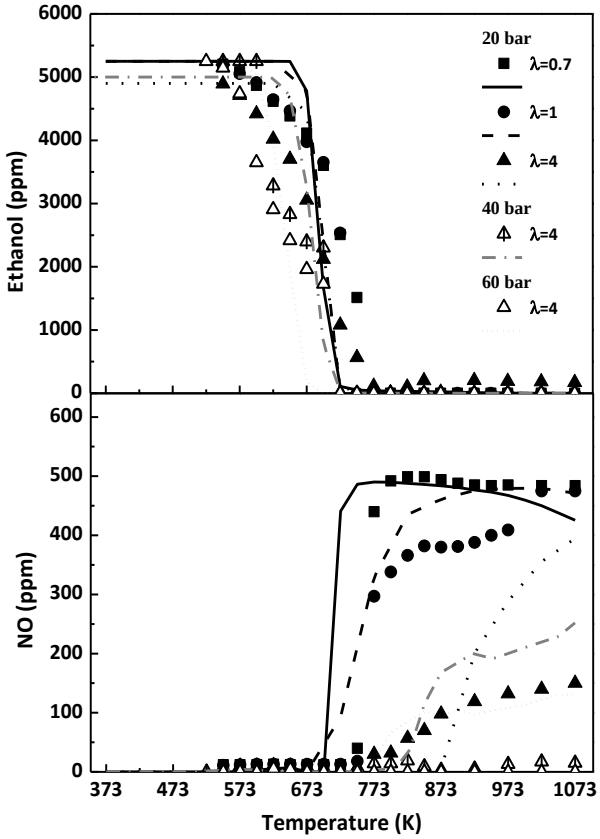

383 **Figure 6.** Influence of the air excess ratio and pressure on the concentration profiles of ethanol (top) and NO

384 (bottom) for the conditions named as sets 10, 13 and 16-18 in Table 1.

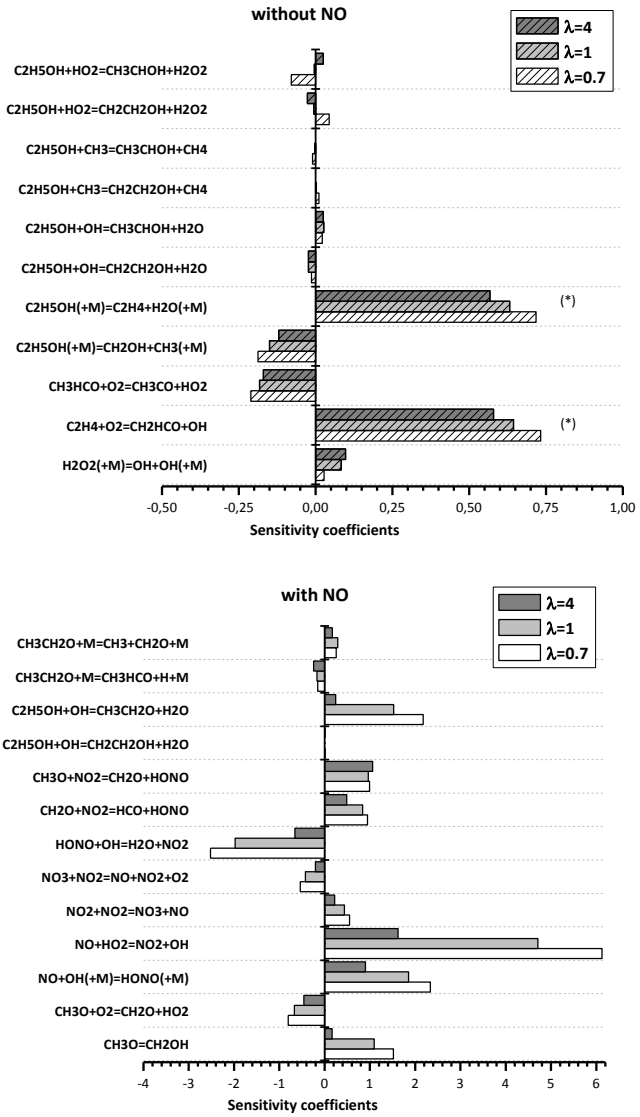

385

386 **Figure 7.** Sensitivity analysis for CO for different air excess ratios and 20 bar. Top: in the absence of NO (at

387 698 K). Bottom: in the presence of NO (at 648 K). (*) The sensitivity coefficients have been divided by two.

388

List of Supplementary Materials (L. Marrodán et al., High-pressure ethanol oxidation and its interaction with NO *Fuel 2017*)

1/ Kinetic model: mechanism (CHEMKIN file)

2/ Supplementary material (PDF file)

3/ Experimental data (Excel file)